

Supplementary Materials

Investigation of Thermal Behaviour of Layered Double Hydroxides Intercalated with Carboxymethylcellulose Aiming Bio-Carbon Based Nanocomposites

Vagner R. Magri ¹, Alfredo Duarte ¹, Gustavo F. Perotti ^{1,2} and Vera R.L. Constantino ^{1,*}

¹ Departamento de Química Fundamental, Instituto de Química, Universidade de São Paulo (USP), Av. Prof. Lineu Prestes 748, CEP 05508-000, São Paulo, SP, Brazil; vrmagri@usp.br (V.R.M.); aduarte@iq.usp.br (A.D.); gustavoperotti@ufam.edu.br (G.F.P.)

² Instituto de Ciências Exatas e Tecnologia, Universidade Federal do Amazonas (UFAM), Rua Nossa Senhora do Rosário 3863, CEP 69103-128, Itacoatiara, AM, Brazil

* Correspondence: vrlconst@iq.usp.br; Tel.: +55-11-3091-9152

Received: 31 March 2019; Accepted: 27 May 2019; Published: 1 June 2019

Table S1. Interplanar distances d_{hkl} and 2θ ($\text{CuK}\alpha$) values from X-ray diffraction data of LDH-CO₃ and LDH-CMC. The indexation of diffraction peaks is based on R-3m space group.

<i>hkl</i>	Zn ₂ Al-CO ₃		Mg ₂ Al-CO ₃		Zn ₂ Al-CMC		Mg ₂ Al-CMC	
	2θ (°)	d (nm)	2θ (°)	d (nm)	2θ (°)	d (nm)	2θ (°)	d (nm)
(003)	11.729	0.754	11.570	0.765	3.543	2.492	5.047	1.750
(006)	23.562	0.378	23.290	0.382	6.156	1.435	10.578	0.836
(009)	35.809	0.251	--	--	10.130	0.873	--	--
(101)	33.968	0.264	--	--	--	--	--	--
(012)	34.675	0.259	34.905	0.257	33.930	0.264	35.270	0.254
(104)	37.379	0.241	--	--	--	--	--	--
(015)	39.300	0.229	39.406	0.229	--	--	--	--
(107)	44.078	0.205	--	--	--	--	--	--
(018)	46.866	0.194	46.788	0.194	--	--	--	--
(0012)	48.145	0.189	--	--	--	--	--	--
(1010)	53.090	0.172	52.899	0.173	--	--	--	--
(0111)	56.491	0.163	56.242	0.164	--	--	--	--
(110)	60.306	0.153	60.853	0.152	60.547	0.153	61.208	0.151
(113)	61.663	0.150	62.161	0.149	--	--	--	--
(1013)	63.823	0.146	63.395	0.147	--	--	--	--
(116)	65.645	0.142	66.054	0.141	--	--	--	--
(0114)	67.751	0.138	--	--	--	--	--	--
d ₀₀₃ (nm)		0.754		0.765		2.492		1.750
c (nm) *		2.262		2.295		7.476		5.250
<i>a</i> and <i>b</i> (nm)		0.306		0.304		0.306		0.302

(*) *c* parameter was calculated considering $c = 3 \times d_{003}$; (#) *a/b* parameter was calculated considering $a = 2 \times d_{110}$.

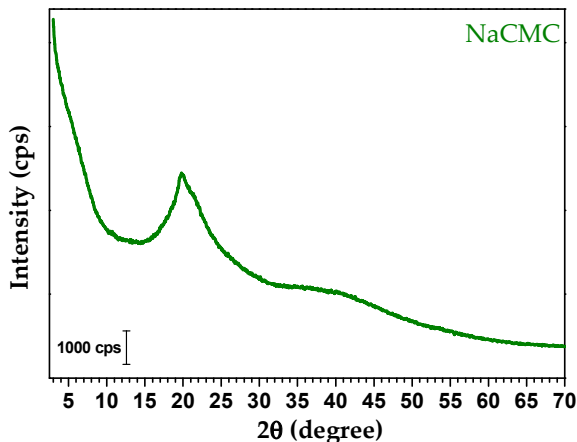


Figure S1. XRD pattern of sodium carboxymethylcellulose (NaCMC).

FTIR-ATR and Raman Spectra of LDH-CO₃ Samples

The infrared spectra of Zn₂Al-CO₃ and Mg₂Al-CO₃ are presented in Figure 4 in the main text. The broad band in the region between 3700–3100 cm⁻¹ can be attributed to the stretching vibrations of the hydroxyl groups (vOH) from inorganic layer and the water molecules hydrogen-bonded. The shoulder at 3020 cm⁻¹ region is assigned to vOH of H₂O molecules interacting with CO₃²⁻ by hydrogen bonding while the band at 1600–1635 cm⁻¹ is related to the in-plane bending vibration of H₂O [1–4]. The bands of carbonate ions are observed in the region of 1354 cm⁻¹ (antisymmetric stretching, v₃), 860 cm⁻¹ (out of plane, v₂) and 680 cm⁻¹ (in-plane bending, v₄) [1,4,5]. In the region below 1000 cm⁻¹, the spectra show bands attributed to the lattice vibrations modes of the groups M-O-M and HO-M-OH (M = Zn²⁺, Mg²⁺, Al³⁺). The strong band at 760 cm⁻¹ is attributed to antisymmetric bending vibrations of HO-Al-OH groups [3,6] while the band at 674 cm⁻¹, only observed in Mg₂Al-CO₃ spectrum, can be attributed to antisymmetric bending of HO-Mg-OH groups.

FT-Raman spectra of Zn₂Al-CO₃ and Mg₂Al-CO₃ are also presented in Figure 4 in the main text. The broad band in the 3140 cm⁻¹ region is attributed to the stretching vibrations of the layer hydroxide ions (vOH) and the H₂O molecules. The band at 1060 cm⁻¹ is assigned to symmetric stretching (v₁) of carbonate anion [1,5]. The band at 495 cm⁻¹ is attributed to the antisymmetric stretching lattice of M²⁺-O-Al [3] and shown to be dependent of M²⁺ cation, being more intense to Zn²⁺ possibly owing to its higher polarizability than Mg²⁺. A tentative attribution of the main vibrational bands is presented in Table S2.

Table S2. Vibrational data of $\text{Zn}_2\text{Al}-\text{CO}_3$ and $\text{Mg}_2\text{Al}-\text{CO}_3$ samples.

$\text{Zn}_2\text{Al}-\text{CO}_3$		$\text{Mg}_2\text{Al}-\text{CO}_3$		Tentative Attribution	Reference
FTIR	Raman	FTIR	Raman		
3700–3100	3143	3700–3100	3143	νOH (M-OH and H ₂ O)	[1–4]
3026 (sh)	--	3026 (sh)	--	νOH (H ₂ O---CO ₃ ²⁻)	
1400(sh)	--	1400(sh)	--	$\nu_3\text{CO}_3^{2-}$	[1,4,5]
1351	--	1358	--	$\nu_3\text{CO}_3^{2-}$	
1632	--	1600	--	$\delta_{ip}\text{H}_2\text{O}$	[1–4]
1058	1060	1058	1059	$\nu_1\text{CO}_3^{2-}$	[1,4,5]
946 (sh)	--	946 (sh)	--	$\delta\text{Al-O-H}$	[6]
863 (sh)	--	863 (sh)	--	$\nu_2\text{CO}_3^{2-}$	[1,4,5]
760	--	760	--	$\delta\text{as}(\text{HO-Al-OH})_l$	[3,6]
--	698	688 (sh)	698	$\nu_4\text{CO}_3^{2-}$	[1,4,5]
--	--	674	--	$\delta\text{as}(\text{HO-Mg-OH})_l$	[3]
630	--	630 (sh)	--	$\delta_s(\text{HO-Al-OH})_l$	[3]
556	--	558	--	$\text{vas}(\text{M}^{2+}\text{-O-Al})_L$	[3]
--	565	--	565	$\text{vs}(\text{M}^{2+}\text{-O-Al})_L$	[3]
525	--	--	--	$\delta\text{as}(\text{HO-Zn}^{2+}\text{-OH})_l$	[4]
--	495	--	483	$\text{vs}(\text{M}^{2+}\text{-O-Al})_L$	[3]
423	--	440 (sh)	--	$\delta\text{as}(\text{M}^{2+}\text{-O-Al})_L$	[3]
--	155	--	151	$\delta(\text{O-M}^{2+}\text{-O})$	[7]

ν = stretching; δ = bending; s: symmetric; as: antisymmetric; ip: in plane; sh: shoulder; L: lattice; l = vibrations; M²⁺ = divalent cation; ν_1 = symmetric stretching; ν_3 = antisymmetric stretching; ν_2 = bending out of plane; ν_4 = bending in plane.

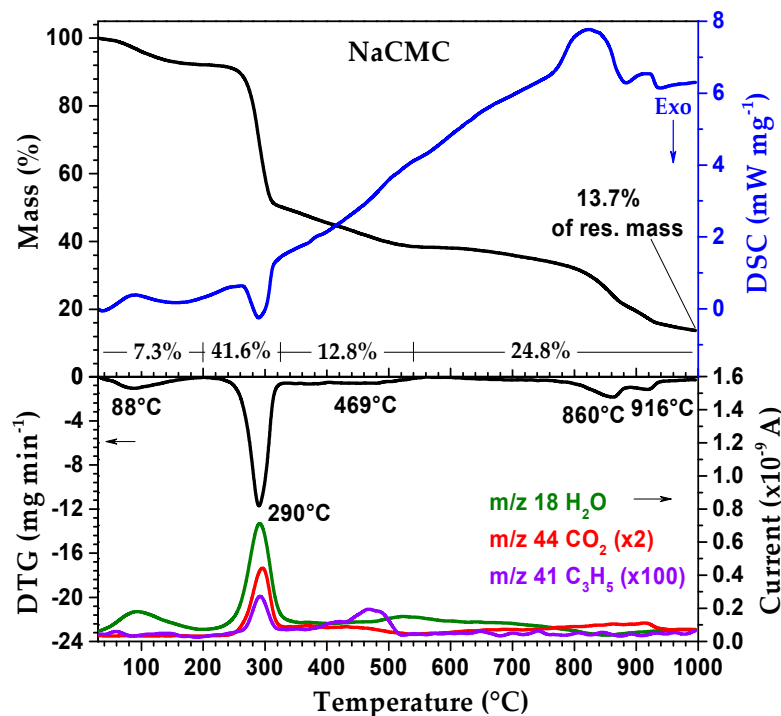
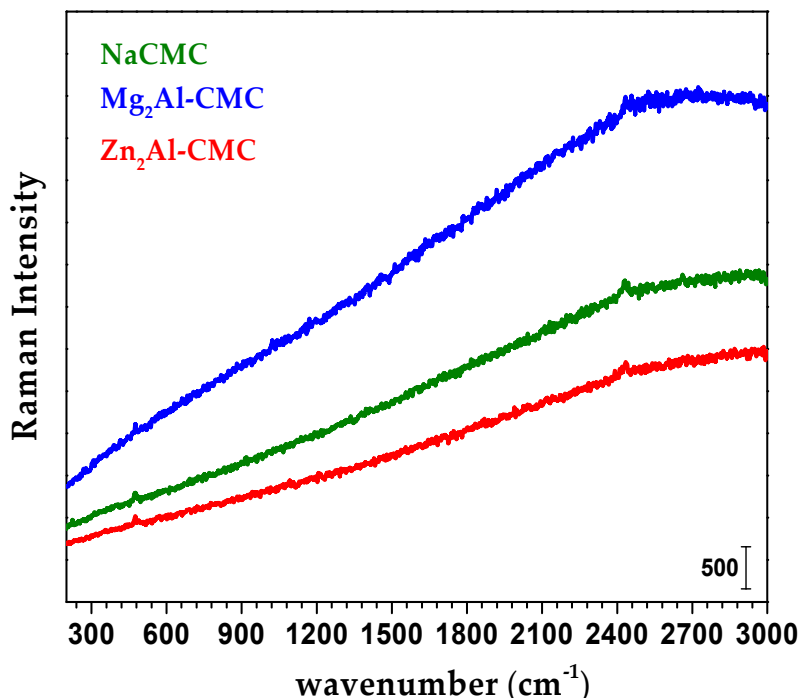


Figure S2. TG-DSC (up) and DTG-MS (down) curves of sodium carboxymethylcellulose (NaCMC) under N₂ atmosphere.

Table S3. Chemical analysis data and proposed formula for LDH-CO₃ and LDH-CMC samples.

Sample	Proposed Formula [§]	%C [†]	%H ₂ O [*]
Mg ₂ Al-CO ₃	[Mg _{2.00} Al(OH) _{6.00}](CO ₃) _{0.50} ·2.43 H ₂ O	-- (2.39)	17.40 (17.40)
Zn ₂ Al-CO ₃	[Zn _{2.14} Al(OH) _{6.28}](CO ₃) _{0.50} ·3.28 H ₂ O	-- (1.66)	16.30 (16.30)
Mg ₂ Al-CMC	[Mg _{2.18} Al(OH) _{6.36}](RU) _{1.15} (Cl) _{0.20} ·2.36 H ₂ O	20.80 (20.90)	8.80 (8.68)
Zn ₂ Al-CMC	[Zn _{1.84} Al(OH) _{5.68}](RU) _{1.43} (Na _{0.23} RU _{0.33})·2.88 H ₂ O	22.80 (22.80)	7.56 (7.56)

[§] M²⁺/Al³⁺ metal ratio was calculated from ICP OES; [†] calculated from carbon elemental analysis; ^{*} calculated from TG curves; RU: (C₆H₁₀O₅)(C₂H₂O₂)_{0.7}; () values obtained based on the proposed formula.

**Figure S3.** Raman spectra ($\lambda_{\text{exc.}} = 532 \text{ nm}$) of NaCMC and LDH-CMC samples.

FTIR-ATR Spectra of LDH-CO₃ Calcined Samples

FTIR-ATR spectra of calcined samples (MMO/C nanocomposites) are shown in Figure S4. LDH-CO₃ samples submitted to the same conditions than LDH-CMC materials were analysed by this vibrational technique for comparison. Zn₂Al-CO₃ sample heated at 500 °C presents two remarkable bands at 1532 cm⁻¹ and 1388 cm⁻¹ attributed to the split of v₃ vibrational mode of carbonate anion. These vibrational bands present Δv equal to 144 cm⁻¹ and can be assigned to CO₃²⁻ ion coordinated to the layer metal cations [8]. Coordination process also activates the v₁ mode of carbonate. The v₃ bands are also noticed with low intensity in the spectrum of Zn₂Al-CO₃ calcined at 600 °C but are practically absent in FTIR-ATR spectra of samples calcined at 800 and 1000 °C. Hence, carbonate coordination to metal sites of LDH layers can explain the thermal profile observed above 500 °C for Zn₂Al-CO₃ sample (Figure 5 in the main text). Mg₂Al-CO₃ spectra also show bands at 1600–1350 cm⁻¹ region but with different shape that can be attributed mainly to absorption of atmospheric carbon dioxide at high basic surface of calcined samples [9,10] (spectra were recorded in *ex situ* mode). In general, bands observed below 900 cm⁻¹ are assigned to vibrational modes of M-O bonds, as presented in Table S2.

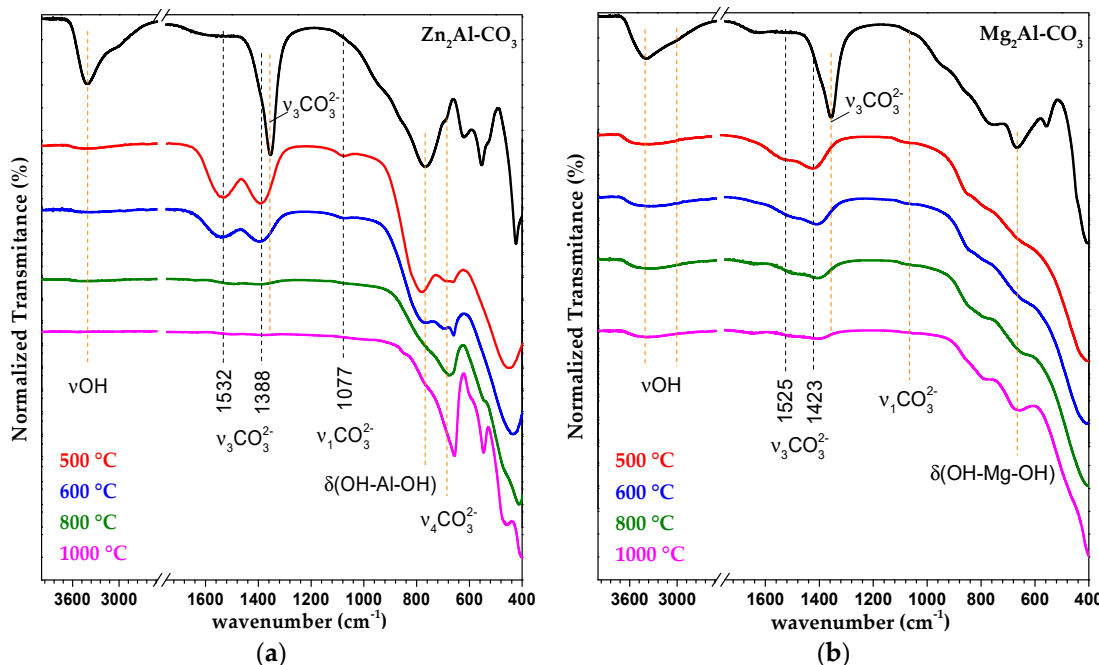


Figure S4. FTIR-ATR spectra of $\text{Zn}_2\text{Al}-\text{CO}_3$ (a) and $\text{Mg}_2\text{Al}-\text{CO}_3$ (b) samples calcined at 500, 600, 800 and 1000 °C under N_2 atmosphere.

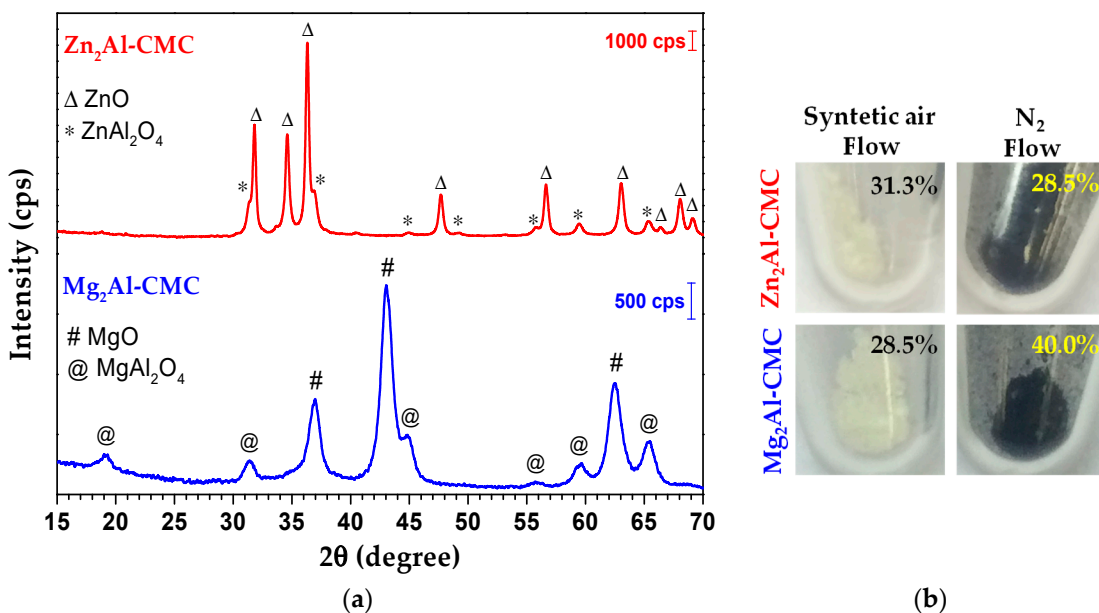


Figure S5. XRD patterns of $\text{M}_2\text{Al}-\text{CMC}$ samples calcined at 1000 °C under synthetic air (a). Pictures of $\text{M}_2\text{Al}-\text{CMC}$ samples calcined at 1000 °C under synthetic air or nitrogen atmosphere, indicating the percentage of residue after each heating process (b).

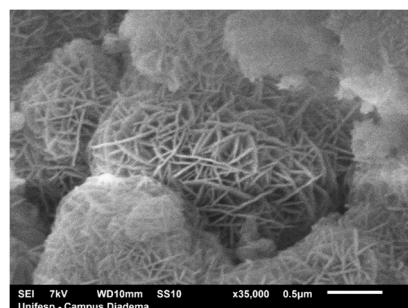


Figure S6. SEM image of $\text{Mg}_2\text{Al}-\text{CO}_3$ sample.

Thermodynamic Considerations about Carbothermic Reaction

Thermodynamic parameters were used to calculate the Gibbs free energy of carbothermic reaction ($\Delta_{\text{R}}G^\circ$) between graphite carbon and metal oxides (ZnO and MgO). The standard molar thermodynamic parameters of each substance at 25 °C are shown in Table S4 and the results are presented in Table S5.

Table S4. Standard molar thermodynamic parameters of substances at 25 °C.

Substance	State	$\Delta_f H^\circ \text{ kJ mol}^{-1}$	$S^\circ \text{ J K}^{-1} \text{ mol}^{-1}$	$\Delta_f G^\circ \text{ kJ mol}^{-1}$	Reference
C(graf.)	s	0	5.74(10)	0	[11]
CO	g	-110.53(17)	197.660(4)	-137.16	[11]
ZnO	s	-348.280	43.64	-318.30	[12]
Zn ⁰	s	0	41.63(15)	0	-
Zn ⁰	g	130.40(40)	160.990(4)	95.14	[11,12]
MgO	s	-601.6	26.95	-569.3	[11,12]
Mg ⁰	s	0	32.67(10)	0	-
Mg ⁰	g	147.1(8)	148.648(3)	113.10	[11]

Table S5. Standard molar thermodynamic values for the carbothermic reaction between graphitic carbon and zinc or magnesium oxides at 25 °C. Values calculated from data presented in Table S4.

Chemical Equation of Reaction	$\Delta_{\text{R}} H^\circ \text{ kJ mol}^{-1}$	$\Delta_{\text{R}} S^\circ \text{ J K}^{-1} \text{ mol}^{-1}$	$\Delta_{\text{R}} G^\circ \text{ kJ mol}^{-1}$	$T_{\text{RS}} (\text{°C})$	$T_{\text{exp}}^* (\text{°C})$
$\text{ZnO}_{(\text{s})} + \text{C}_{(\text{s})} \rightarrow \text{Zn}^0_{(\text{v})} + \text{CO}_{(\text{g})}$	368.15	309.26	276.29	917	>880
$\text{MgO}_{(\text{s})} + \text{C}_{(\text{s})} \rightarrow \text{Mg}^0_{(\text{v})} + \text{CO}_{(\text{g})}$	638.28	313.62	545.24	1762	-

T_{RS} = temperature of reaction spontaneity; * taken from the thermal analysis result (Figure 5).

Carbothermic reactions are obviously not spontaneous at 25 °C but the entropy ($\Delta_{\text{R}}S^\circ$) is positive and the reactions tend to become spontaneous with increasing of the temperature. The value of temperature to promote a spontaneous carbothermic reaction (T_{RS}) was estimated considering that $\Delta_{\text{R}}H^\circ$ and $\Delta_{\text{R}}S^\circ$ do not change significantly and the equilibrium conditions. The calculated T_{RS} value suggests that carbothermic reaction for ZnO reduction tends to become spontaneous above 917 °C, a value very close to that one observed in this work (880 °C). For MgO, the T_{RS} value is much higher (1762 °C) than for ZnO. The results of calculations agree with the processes experimentally observed.

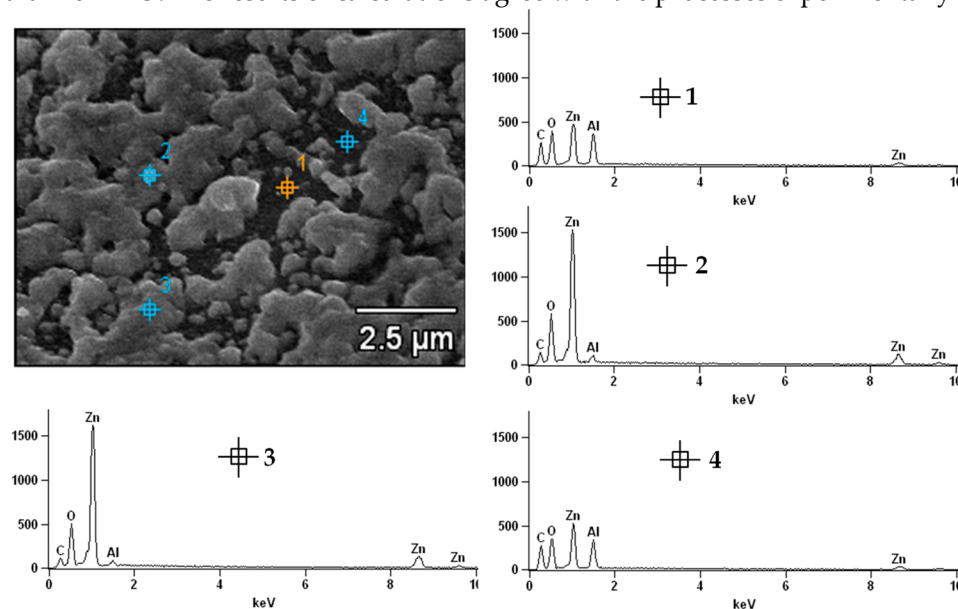


Figure S7. EDS spectra of Zn₂Al-CMC sample pyrolyzed at 800 °C.

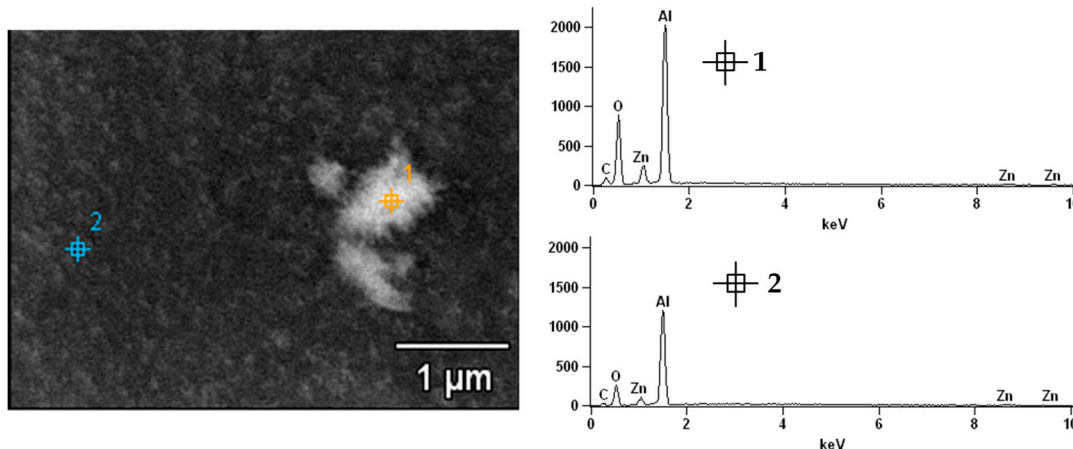


Figure S8. EDS spectra of Zn₂Al-CMC sample pyrolyzed at 1000 °C.

References

1. Labajos, F.M.; Rives, V.; Ulibarri, M.A. Effect of hydrothermal and thermal treatments on the physicochemical properties of Mg-Al hydrotalcite-like materials. *J. Mater. Sci.* **1992**, *27*, 1546–1552.
2. Kloprogge, J.T.; Frost, R.L. Fourier Transform Infrared and Raman Spectroscopic Study of the Local Structure of Mg-, Ni-, and Co-Hydrotalcites. *J. Solid State Chem.* **1999**, *146*, 506–515.
3. Kaguny, W.; Baddour-Hadjean, R.; Kooli, F.; Jones, W. Vibrational modes in layered double hydroxides and their calcined derivatives. *Chem. Phys.* **1998**, *236*, 225–234.
4. Kloprogge, J.T.; Hickey, L.; Frost, R.L. The effects of synthesis pH and hydrothermal treatment on the formation of zinc aluminum hydrotalcites. *J. Solid State Chem.* **2004**, *177*, 4047–4057.
5. Kloprogge, J.T.; Wharton, D.; Hickey, L.; Frost, R.L. Infrared and Raman study of interlayer anions CO₃²⁻, NO₃⁻, SO₄²⁻ and ClO₄⁻ in Mg/Al-hydrotalcite. *Am. Mineral.* **2002**, *87*, 623–629.
6. Theo Kloprogge, J.; Frost, R.L. Infrared emission spectroscopic study of the dehydroxylation of synthetic Mg/Al and Mg/Zn/Al-hydrotalcites. *Phys. Chem. Chem. Phys.* **1999**, *1*, 1641–1647.
7. Gil, O.M.; Rocha, M.A.; Constantino, V.R.L.; Koh, I.H.J.; de Faria, D.L.A. Modified drug release system based on Sulindac and layered double hydroxide: An in vivo Raman investigation. *Vib. Spectrosc.* **2016**, *87*, 60–66.
8. Greenaway, A.M.; Dasgupta, T.P.; Koshy, K.C.; Sadler, G.G. A correlation between infrared stretching mode absorptions and structural angular distortions for the carbonato ligand in a wide variety of complexes. *Spectrochim. Acta Part A Mol. Spectrosc.* **1986**, *42*, 949–954.
9. Constantino, V.R.L.; Pinnavaia, T.J. Basic Properties of Mg²⁺_{1-x}Al³⁺_x Layered Double Hydroxides Intercalated by Carbonate, Hydroxide, Chloride, and Sulfate Anions. *Inorg. Chem.* **1995**, *34*, 883–892.
10. Prinetto, F.; Ghiotti, G.; Giuria, V.P.; Durand, R.; Tichit, D. Investigation of Acid-Base Properties of Catalysts Obtained from Layered Double Hydroxides. *J. Phys. Chem. B* **2000**, *104*, 11117–11126.
11. Speight, J. *Lange's Handbook Of Chemistry*, 16th ed.; 2005; ISBN 9780071432207.
12. Atkins, P.W.; Paula, J. de *Físico-química*; vol. 1, 9th ed.; LTC: Rio de Janeiro, 2010; ISBN 978-85-216-2104-1.



© 2019 by the authors. Licensee MDPI, Basel, Switzerland. This article is an open access article distributed under the terms and conditions of the Creative Commons Attribution (CC BY) license (<http://creativecommons.org/licenses/by/4.0/>).